Biomaterials xxx (2012) 1–9

Contents lists available at SciVerse ScienceDirect

Biomaterials

journal homepage: www.elsevier.com/locate/biomaterials

Differential responses of osteoblast lineage cells to nanotopographically-modified, microroughened titanium–aluminum–vanadium alloy surfaces

Rolando A. Gittens [a], Rene Olivares-Navarrete [b], Taylor McLachlan [a], Ye Cai [a], Sharon L. Hyzy [c], Jennifer M. Schneider [d], Zvi Schwartz [b], Kenneth H. Sandhage [a,e], Barbara D. Boyan [a,b,c,*]

[a] School of Materials Science and Engineering, Georgia Institute of Technology, Atlanta, GA, USA
[b] Wallace H. Coulter Department of Biomedical Engineering at Georgia Tech and Emory University, Georgia Institute of Technology, Atlanta, GA, USA
[c] School of Biology, Georgia Institute of Technology, Atlanta, GA, USA
[d] Titan Spine LLC, Mequon, WI, USA
[e] School of Chemistry and Biochemistry, Georgia Institute of Technology, Atlanta, GA, USA

ARTICLE INFO

Article history:
Received 6 July 2012
Accepted 24 August 2012
Available online xxx

Keywords:
Metallic implants
Osteointegration
Titanium–aluminum –vanadium alloy
Bone
Nanostructures
Osteoblast differentiation

ABSTRACT

Surface structural modifications at the micrometer and nanometer scales have driven improved success rates of dental and orthopaedic implants by mimicking the hierarchical structure of bone. However, how initial osteoblast-lineage cells populating an implant surface respond to different hierarchical surface topographical cues remains to be elucidated, with bone marrow mesenchymal stem cells (MSCs) or immature osteoblasts as possible initial colonizers. Here we show that in the absence of any exogenous soluble factors, osteoblastic maturation of primary human osteoblasts (HOBs) but not osteoblastic differentiation of MSCs is strongly influenced by nanostructures superimposed onto a microrough Ti6Al4V (TiAlV) alloy. The sensitivity of osteoblasts to both surface microroughness and nanostructures led to a synergistic effect on maturation and local factor production. Osteoblastic differentiation of MSCs was sensitive to TiAlV surface microroughness with respect to production of differentiation markers, but no further enhancement was found when cultured on micro/nanostructured surfaces. Superposition of nanostructures to microroughened surfaces affected final MSC numbers and enhanced production of vascular endothelial growth factor (VEGF) but the magnitude of the response was lower than for HOB cultures. Our results suggest that the differentiation state of osteoblast-lineage cells determines the recognition of surface nanostructures and subsequent cell response, which has implications for clinical evaluation of new implant surface nanomodifications.

1. Introduction

Bone and joint injuries are among the most reported health problems in the United States [1]. Although orthopaedic implants provide a good option for joint replacements, with success rates continually improving, they still have undesirable failure rates in patients who are compromised by disease or age (i.e., patients who are often the ones most in need) [2,3].

Surface topographical modifications at the micrometer and nanometer scales have driven improved success rates for dental implants by mimicking the hierarchical structure of bone associated with regular bone remodeling [4,5]. In this process, damaged bone is resorbed by osteoclasts, which produce resorption lacunae containing high microroughness generated after mineral dissolution under the ruffled border [6], as well as superimposed nanoscale features created by the collagen fibers exposed at the surface [7]. New bone formation by osteoblasts is coupled with these primed surfaces, possibly after recognition of structural and chemical cues [8,9]. Thus, surface topographical modifications have been exploited for implant design in order to achieve direct and intimate contact between the bone and the surface of the implant (osseointegration). Indeed, the beneficial effects of microroughness for bone formation have been well established in the literature [10], and the addition of nanostructures to the implant surface (to mimic more closely the natural structure of bone) has shown promising results *in vitro* [11], *in vivo* [12] and clinically [13,14], validating the biological relevance of nanotopography for bone formation.

Titanium (Ti) and its alloys are widely-used metals for dental and orthopaedic implant applications due to their favorable

* Corresponding author. Institute for Bioengineering and Bioscience, Georgia Institute of Technology, 315 Ferst Drive, NW (Suite 1108), Atlanta, GA 30332-0363, USA. Tel.: +1 404 385 4108; fax: +1 404 894 2291.
E-mail address: barbara.boyan@bme.gatech.edu (B.D. Boyan).

0142-9612/$ – see front matter © 2012 Elsevier Ltd. All rights reserved.
http://dx.doi.org/10.1016/j.biomaterials.2012.08.059

weight-to-strength ratio and good biological performance in bone. Implant surface modifications at the microscale involve adding to, removing from, or deforming material on the bulk metallic substrate (*e.g.*, acid etching, sandblasting) to generate features that are comparable in size or larger than cells [15,16]. More recently, surface nanomodifications have been developed to directly restructure the oxide layer formed on the implant surface using different techniques, such as coatings [17], hydrothermal reactions [18], and surface oxidation [19,20]. The generated oxide nanostructures can then interact with proteins and other small molecules that will eventually influence early cell behavior and long-term osseointegration [21].

The differentiation state required to respond to the surface topographical cues by the initial osteoblast lineage cells (to populate the surface of an implant) remains to be elucidated, with bone marrow mesenchymal stem cells (MSCs) or immature osteoblasts as possible candidates. Several recent studies using MSCs *in vitro* consider these cells as initial colonizers of the implant surface due to their higher mobility and ability to differentiate into osteoblasts and other cell types [22,23]. Many of these studies culture the MSCs using exogenous factors, such as β-glycerophosphate, dexamethasone, and bone morphogenetic protein-2 (BMP-2) [24,25], to force their differentiation into osteoblasts, which could be obscuring the real effects of the surface nanotopography [26]. We have recently demonstrated that human MSCs can differentiate into osteoblasts when cultured on Ti surfaces possessing microscale roughness, even in the absence of these media supplements [27]. However, it is not known if osteogenic differentiation of MSCs is a general response to microrough metal surfaces, including Ti alloys, or if it is specific to commercially pure Ti. How the addition of nanoscale features to a microrough surface will affect such differentiation is also unclear.

The goal of the present study has been to test the hypothesis that nanostructural features on implant surfaces can enhance the osteogenic differentiation of osteoblast-lineage cells in the absence of any exogenous soluble factors. To test this hypothesis, we have superimposed nanostructures on microrough Ti6Al4V surfaces and examined the responses of human MSCs and primary human osteoblasts without the addition of exogenous soluble factors.

2. Materials and methods

2.1. Titanium alloy specimens and surface modification treatments

Titanium alloy rods (ASTM F136 wrought Ti6Al4V ELI alloy for surgical implant applications) 15 mm in diameter were cut into 1.5 mm thick disks and either machined to create a relatively smooth surface (control specimens referred to herein as "sTiAlV" specimens), or double-acid-etched with a proprietary process (Titan Spine LLC, Mequon, WI) to produce a microrough surface (specimens referred to herein as "rTiAlV" specimens). These disk specimens were provided by Titan Spine LLC. Some of the microsmooth (sTiAlV) and microrough (rTiAlV) specimens were further processed using a simple oxidation treatment to superimpose nanostructures on the surface, as described previously [11], to yield nanomodified, microsmooth (NMsTiAlV) or nanomodified, microrough (NMrTiAlV) specimens. This simple oxidation treatment consisted of exposing the samples to flowing (0.85 standard liters per minute) synthetic air (21% O_2, 79% N_2) at 1 atm and 740 °C for relatively short durations. The oxidation treatment was conducted for durations of 45, 90 and 180 min on all of the specimens and, based on qualitative evaluations of secondary electron (SE) images (as discussed below), disks modified for 45 min were chosen for use in cell experiments. All modified and unmodified disks were ultrasonically cleaned in detergent (Micro-90; International Products Corporation, Burlington, NJ) and ultrapure water (Advantage A10; Millipore, Billerica, MA), followed by autoclave sterilization (Model 2540E; Tuttnauer, Hauppauge, NY) for 20 min at 121 °C and 15 PSI before surface characterization and use in cell culture studies.

To confirm the "non-line-of-sight" nature of the nanomodification induced by the oxidation treatment, clinically-available Ti6Al4V spine implants of complex shape that had been exposed to the double acid etch surface modification treatment (Endoskeleton® TT implants; Titan Spine, LLC) were oxidized as described above, and the nanostructures generated on the internal walls of this specimen were compared to those generated on the external surfaces of the disk-shaped NMrTiAlV specimens.

2.2. Surface characterization

2.2.1. Electron microscopy

Surface topography was qualitatively evaluated using a field-emission-gun scanning electron microscope (Ultra 60 FEG-SEM; Carl Zeiss SMT Ltd., Cambridge, UK). Secondary electron (SE) images were recorded using a 5 kV accelerating voltage and 30 μm aperture. Histograms of the diameters of nanoscale protuberances (i.e., the major axis of the nanostructure as determined from top-down views) were generated with image analysis software (ImageJ; NIH Software) using three fields of view from two different samples per specimen type, with at least 150 nanoscale protuberances evaluated per specimen type. In addition, the thickness of the oxide layer formed upon the nano-modification oxidation treatment was evaluated using a transmission electron microscope (TEM, JEM 4000 EX, JEOL, Tokyo, Japan) with an accelerating voltage of 400 kV. Electron transparent cross-sections obtained from the surface regions of the NMsTiAlV specimens were prepared using a focused ion beam system (FEI Nova Nanolab 200 FIB/SEM; FEI, Hillsboro, OR).

2.2.2. Atomic force microscopy (AFM)

Surface measurements at the nanoscale were evaluated using AFM (Nano-R AFM; Pacific Nanotechnology, Santa Clara, CA) in close-contact mode. Analyses were conducted using silicon probes (P-MAN-SICC-O, Agilent Technologies, Santa Clara, CA) with dimensions of 1.14 cm × 0.25 cm^2 and tip radii of up to 10 nm, a nominal force constant of 40 N/m, and a nominal resonance frequency of 300 kHz. Each AFM analysis was performed over a 730 nm × 730 nm specimen area. Two samples of the sTiAlV and NMsTiAlV specimens were scanned three times each, under ambient atmosphere. (Note: because the *z*-height limit of the AFM was 5 μm, the microrough surfaces could not be analyzed by AFM.) The raw data were plane-leveled to remove tilt by applying a numerical second-order correction, and mean values of surface roughness average (S_a) were determined using NanoRule+ software (Pacific Nanotechnology).

2.2.3. Laser confocal microscopy (LCM)

Surface roughness at the microscale was evaluated using a laser confocal microscope (Lext LCM; Olympus, Center Valley, PA). Each LCM analysis was performed over a 644 μm × 644 μm area using a scan height step of 100 nm, a 20X objective, and a cutoff wavelength of 100 μm. Two samples of every specimen type were scanned three times each under ambient atmosphere. Mean values of surface roughness average (S_a) were determined.

2.2.4. X-ray photoelectron spectroscopy (XPS)

Relative atomic concentration and chemical bonding information were obtained from the specimen surfaces by XPS analyses (Thermo K-Alpha XPS; Thermo Fisher Scientific, West Palm Beach, FL). The XPS instrument was equipped with a monochromatic Al-Kα X-ray source ($h\nu$ = 1468.6 eV). The XPS analysis chamber was evacuated to a pressure of 5 × 10^{-8} mbar or lower before collecting XPS spectra. Spectra were collected using an X-ray spot size of 400 μm and pass energy of 100 eV, with 1 eV increments, at a 55° takeoff angle. Two samples of every specimen type were scanned three times each and all values were averaged.

2.2.5. Contact angle measurements

Contact angle measurements were obtained using a goniometer (CAM 100; KSV, Helsinki, Finland) equipped with a digital camera and image analysis software. Ultra-pure water was used as the wetting liquid with a drop size of 4 μL. Sessile drop contact angles of the air–water–substrate interface were measured four times over a period of 20 s, on five different spots in two samples from each specimen type.

2.2.6. X-ray diffraction (XRD) analyses

XRD analyses were conducted using 1.8 kW Cu Kα radiation, a 1° parallel plate collimator, and a ½ divergence slit on an X'Pert PRO Alpha-1 diffractometer (PANalytical, Almelo, The Netherlands). A $\theta - 2\theta$ parafocusing setup was used for grazing-angle (i.e., 2° take-off angle) analyses. All samples were analyzed under ambient atmosphere.

2.3. Cell culture model

Primary human osteoblasts (HOBs) and human mesenchymal stem cells (MSCs) were used for this study. Osteoblasts were isolated from vertebral bone of a 17-year old male that was collected under Institutional Review Board approval from Children's Healthcare of Atlanta and Georgia Institute of Technology, as described previously [28]. Briefly, periosteum and soft tissues were removed from the bone. Bone fragments were washed three times in Hank's balanced salt solution (HBSS; Invitrogen, Carlsbad, CA) containing 1% penicillin-streptomycin (Invitrogen), and digested for 15 min at 37 °C with 0.25% trypsin-ethylenediaminetetraacetic acid (EDTA) (Invitrogen). The digest was discarded to avoid fibroblast contamination. The bone was minced into 1–2 mm^2 pieces and bone chips were placed in a 100 × 20 mm^2 Petri dish (BD, Franklin Lakes, NJ) and cultured in Dulbecco's modified Eagle medium (DMEM; cellgro®, Mediatech, Inc., VA) containing 10% fetal bovine serum (Gibco, Carlsbad, CA) and 1% penicillin–streptomycin. At confluence, the cells were further passaged for experiments and were cultured in

Please cite this article in press as: Gittens RA, et al., Differential responses of osteoblast lineage cells to nanotopographically-modified, microroughened titanium–aluminum–vanadium alloy surfaces, Biomaterials (2012), http://dx.doi.org/10.1016/j.biomaterials.2012.08.059

medium as described above. Human MSCs were purchased from a commercial vendor (Lonza, Walkersville, MD) and grown in MSC Growth Medium (MSCGM, Lonza). All cells were cultured at 37 °C with 5% CO_2 and 100% humidity, and cells from the sixth passage or lower were used. Osteoblasts and MSCs were cultured on tissue culture polystyrene (TCPS) or on the different Ti alloy surfaces (sTiAlV, NMsTiAlV, rTiAlV, NMrTiAlV) at a seeding density of 10,000 cells/cm^2. Cells were fed 24 h after plating and then every 48 h until confluence, as evaluated on the TCPS substrates. At confluence, cells were incubated with fresh medium for 24 h and harvested for assays. Conditioned media were collected, and stored at −80 °C until assayed. Cell layers were washed twice with serum-free medium, released from their substrate by two sequential incubations in 500 μL 0.25% trypsin for 10 min at 37 °C, and counted with a Z1 Coulter particle counter (Beckman Coulter, Brea, CA). Cells were resuspended in 500 μL 0.05% Triton-X-100® and lysed by sonication.

Two different osteoblast differentiation markers were evaluated: alkaline phosphatase-specific activity [orthophosphoric monoester phosphohydrolase, alkaline; E.C. 3.1.3.1], which serves as an early differentiation marker; and osteocalcin content in the conditioned medium as a late differentiation marker. Cellular alkaline phosphatase activity was assayed in the cell lysate as the release of *p*-nitrophenol from *p*-nitrophenylphosphate at pH 10.2, and normalized to total protein content (BCA Protein Assay Kit; Pierce Biotechnology Inc., Rockford, IL) as previously described [29]. Osteocalcin levels in the conditioned media were measured using a commercially-available radioimmunoassay kit (Human Osteocalcin RIA Kit, Biomedical Technologies, Stoughton, MA) as described previously [30] using an LS1500 gamma counter (Perkin Elmer, Waltham, CA).

The conditioned media were also assayed for protein levels of local factors important for bone development. Osteoprotegerin (OPG), a cytokine that works as a decoy receptor for "receptor activator for nuclear factor κB ligand" (RANKL) to inhibit osteoclastogenesis, was measured using enzyme-linked immunosorbent assay (ELISA) kits (DY805 Osteoprotegerin DuoSet, R&D Systems, Minneapolis, MN). Vascular endothelial growth factor (VEGF), a growth factor involved in vasculogenesis and angiogenesis, was also measured using an ELISA kit (DY293B VEGF DuoSet, R&D Systems).

2.4. Statistical analysis

Data from experiments evaluating the surface characteristics of the substrates are presented as the mean ± one standard deviation (SD) of all the measurements performed on different samples of the same specimen type. Data from experiments examining cell response are presented as mean ± standard error (SE) for six independent cultures per variable. All experiments were repeated at least twice to ensure the validity of the observations, and the results from individual experiments are presented. Data were evaluated by analysis of variance, and significant differences between groups were determined using Tukey's modification of Student's *t*-test. A p value below 0.05 was considered to indicate a statistically-significant difference.

3. Results

3.1. Characterization of nanomodified surfaces

SE images of the original sTiAlV and rTiAlV surfaces revealed that both were relatively smooth at the nanoscale, with some sub-microscale features left from the machining or double-acid-etch treatment (Fig. 1A and B). However, the surfaces of the titanium alloy specimens that had received the 740 °C oxidation treatment for 45 min (specimens NMsTiAlV and NMrTiAlV) possessed high and homogeneous coverages of nanoscale protuberances (referred to herein simply as nanostructures) with diameters that ranged between 20 and 180 nm (Fig. 1C and D). Statistical image analyses (histograms are shown in Fig. 1E and F) indicated that the average diameters of the nanostructures on the NMsTiAlV and NMrTiAlV surfaces were 73 nm and 61 nm, respectively. SE images from oxidized spine implants that had received the same oxidation treatment revealed that similar nanostructural features were generated on the internal walls as well as external surfaces, confirming the "non-line-of-sight" nature of this surface modification treatment (Fig. 2).

SEM analyses of Ti alloy surfaces exposed to the same oxidation temperature and atmosphere (740 °C, 21% O_2/79% N_2, 1 atm) but for longer times of 90 or 180 min revealed the presence of similar nanostructures (Suppl. Fig. 1), although some coalescence of the nanostructures and a few visible regions of spallation were occasionally observed. Thus, 45 min was selected as the preferred oxidation time for subsequent characterization and cell experiments involving the titanium alloy specimens.

The apparent increase in the nanoscale roughness of the titanium alloy surfaces detected by electron microscopy after the oxidation treatment was confirmed by AFM analyses (Fig. 3A), which revealed significant enhancements in the values of the average nanoscale roughness (6.1 ± 4.3 μm on sTiAlV surfaces compared to 17.0 ± 4.5 μm on NMsTiAlV surfaces). As expected, laser confocal microscopic analyses (Fig. 3A) also revealed that the microroughness of the rTiAlV and NMrTiAlV specimens (as

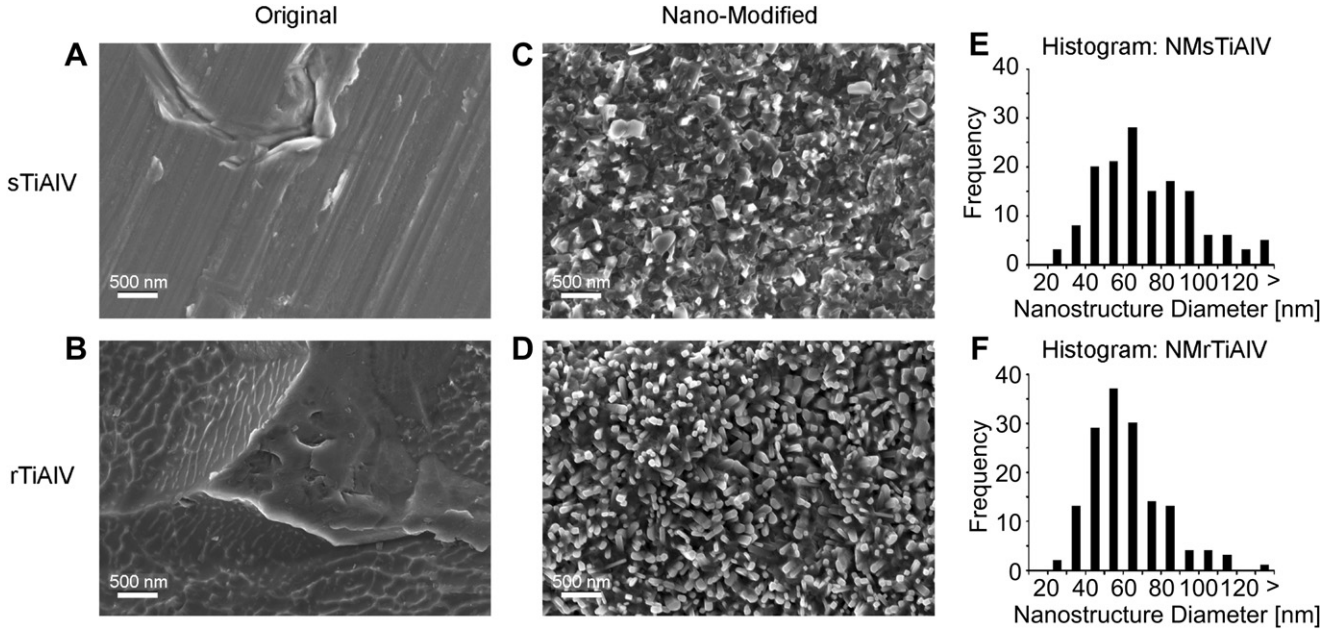

Fig. 1. SE images and image analyses of the Ti alloy surfaces used for *in vitro* cell studies. (A) Microsmooth (sTiAlV) and (B) microrough (rTiAlV) surfaces were relatively smooth at the nanoscale, with some sub-microscale features. After the nanomodification oxidation treatment for 45 min, (C) NMsTiAlV and (D) NMrTiAlV surfaces possessed high and homogeneous surface area coverage of nanostructures. Image analyses of the (E) NMsTiAlV and (F) NMrTiAlV surfaces revealed that the nanostructure diameter (when viewed from above by SEM analyses) ranged between 20 and 180 nm, with average values of 73 nm and 61 nm, respectively.

Please cite this article in press as: Gittens RA, et al., Differential responses of osteoblast lineage cells to nanotopographically-modified, microroughened titanium–aluminum–vanadium alloy surfaces, Biomaterials (2012), http://dx.doi.org/10.1016/j.biomaterials.2012.08.059

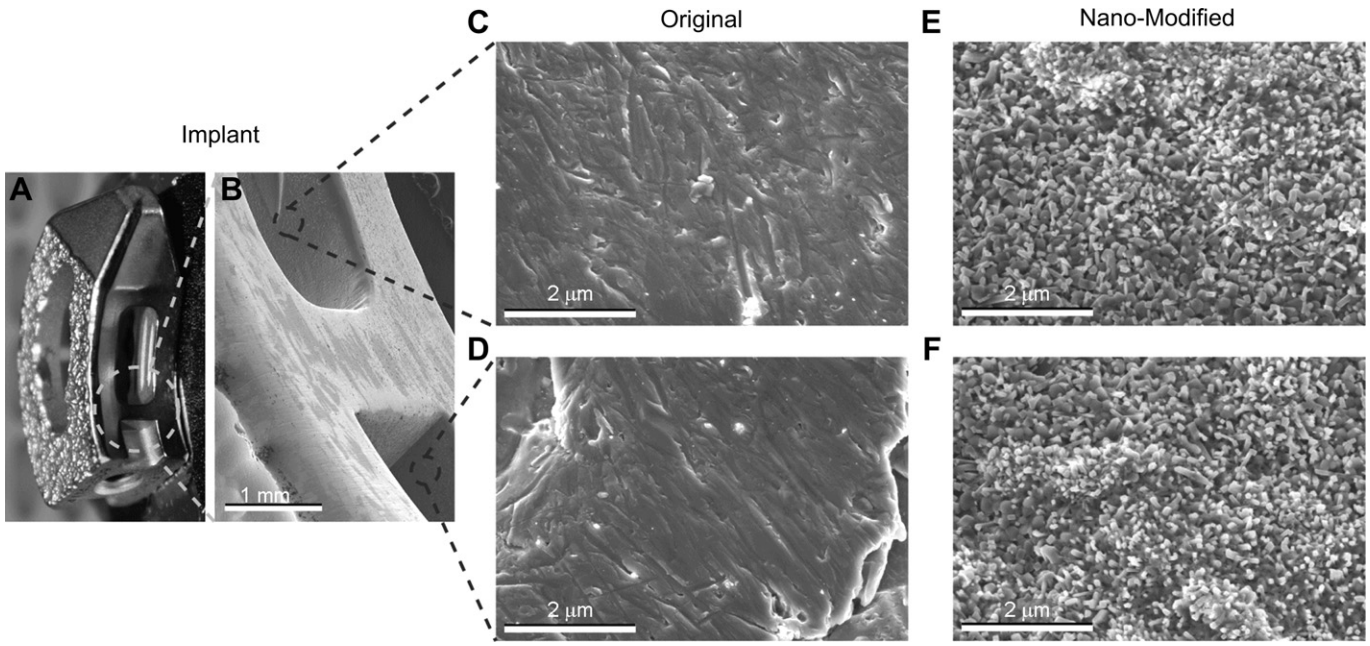

Fig. 2. (A) Optical and (B–D) SE images of the surface nanostructural modification applied to clinically relevant Ti alloy spine implants. (A, B) Low magnification images show the complex design of the device. (C, D) High magnification images of the unmodified implant reveal that the surface was relatively smooth at the micro- and nanoscales. Conversely, (E, F) high magnification images of the nanomodified implant surface display homogeneous coverage of nanostructures throughout exposed and non-line-of-sight areas.

indicated by the microscale surface roughness average, S_a) was significantly higher than for the specimens that had not been acid etched (sTiAlV and NMsTiAlV). However, such surface microroughness did not appear to significantly inhibit the generation of surface nanostructures during the subsequent oxidation treatment (Fig. 1). The oxidation treatment used to enhance the nanoscale roughness also did not significantly affect the microscale roughness of the rTiAlV specimens.

The nanostructural modification of the surface occurred via oxidation of the Ti alloy specimens. TEM evaluation (Fig. 3B) of the NMsTiAlV sample revealed a conformal, but porous oxide layer that was up to 1600 nm thick. (Note: sample processing during preparation of the FIB cross-sections for TEM evaluation removed nanostructural features found on the top-down SE images, as shown in Suppl. Fig. 2). Grazing-angle XRD analysis (Fig. 3C) of this oxidized alloy specimen revealed the presence of polycrystalline TiO_2, with rutile (powder diffraction card No. 21-1276) as the predominant polymorph and some anatase (powder diffraction card No. 21-1272) along with polycrystalline α-Ti (powder diffraction card No. 44-1294) from the underlying alloy. Diffraction peaks for the latter phase and β-Ti (powder diffraction card No. 44-1288) were also detected in the unoxidized sTiAlV specimen. Distinct diffraction peaks for aluminum oxide polymorphs were not detected. The oxidation treatment did not result in a dramatic change in the wettability of the surface by water, as measured by sessile-drop contact angle (Fig. 3D).

Nanoscale modification of Ti alloy surfaces by the oxidation heat treatment affected the surface chemistry of the specimens (Fig. 4). The elemental compositions of the original sTiAlV and rTiAlV surfaces were similar, with Ti, O and C as the main components, and only small amounts of Al and no detectable V present at the surface. However, the surface chemical compositions of the NMsTiAlV and NMrTiAlV specimens were altered after the oxidation treatment, with lower concentrations of Ti and C, and significantly higher concentrations of Al, on the oxidized surfaces, respectively, than for the starting alloy specimens. A larger decrease in Ti concentration and increase in Al concentration were observed after oxidation of the rTiAlV specimen than after oxidation of the sTiAlV specimen.

3.2. Osteoblast lineage cell response to nanomodified surfaces

3.2.1. Osteoblast response

Osteoblastic maturation of HOBs was highly sensitive to the generated nanostructures superimposed onto microrough Ti alloy surfaces in the absence of any exogenous soluble factors. Osteoblast cell number (Fig. 5A), which decreases in differentiated cells due to a transcriptionally-restricted transition between proliferation and differentiation, was lower on the microrough surfaces, with the lowest levels on the combined microrough and nanostructured NMrTiAlV surfaces. At the same time, alkaline phosphatase specific activity (Fig. 5B) and osteocalcin production (Fig. 5C) were higher on the microrough alloy surfaces when compared to the microsmooth alloy surfaces. Additionally, alkaline phosphatase specific activity had a 2.5-fold increase, while osteocalcin production had a synergistic 8.5-fold increase on the NMrTiAlV specimens when compared to the rTiAlV specimens. The increase in differentiation markers on microrough surfaces was also coupled with higher levels of the anti-osteoclastogenesis factor osteoprotegerin (Fig. 5D) and the angiogenic factor VEGF (Fig. 5E). In the case of osteoprotegerin levels, no appreciable difference between rTiAlV and NMrTiAlV specimens was observed, while a 5-fold synergistic increase in VEGF production was observed for the NMrTiAlV surfaces relative to rTiAlV surfaces.

3.2.2. MSC response

MSC numbers (Fig. 5F) were 0.7-fold lower on the nanomodified NMsTiAlV specimens than for the starting sTiAlV specimens, and the cell number decreased further for the microrough rTiAlV specimens, with the lowest levels observed for the nanomodified NMrTiAlV specimens (0.7-fold vs. rTiAlV). However, although osteoblastic differentiation of MSCs was affected by microstructure, it was not responsive to culture on nanomodified surfaces. Alkaline phosphatase specific activity (Fig. 5G) was 1.9-fold higher in cells cultured on microrough rTiAlV specimens compared to microsmooth sTiAlV specimens, as well as 1.3-fold higher than for the micro/nanostructured NMrTiAlV specimens. Osteocalcin levels (Fig. 5H) were also higher on the rTiAlV specimens than on the

Please cite this article in press as: Gittens RA, et al., Differential responses of osteoblast lineage cells to nanotopographically-modified, microroughened titanium–aluminum–vanadium alloy surfaces, Biomaterials (2012), http://dx.doi.org/10.1016/j.biomaterials.2012.08.059

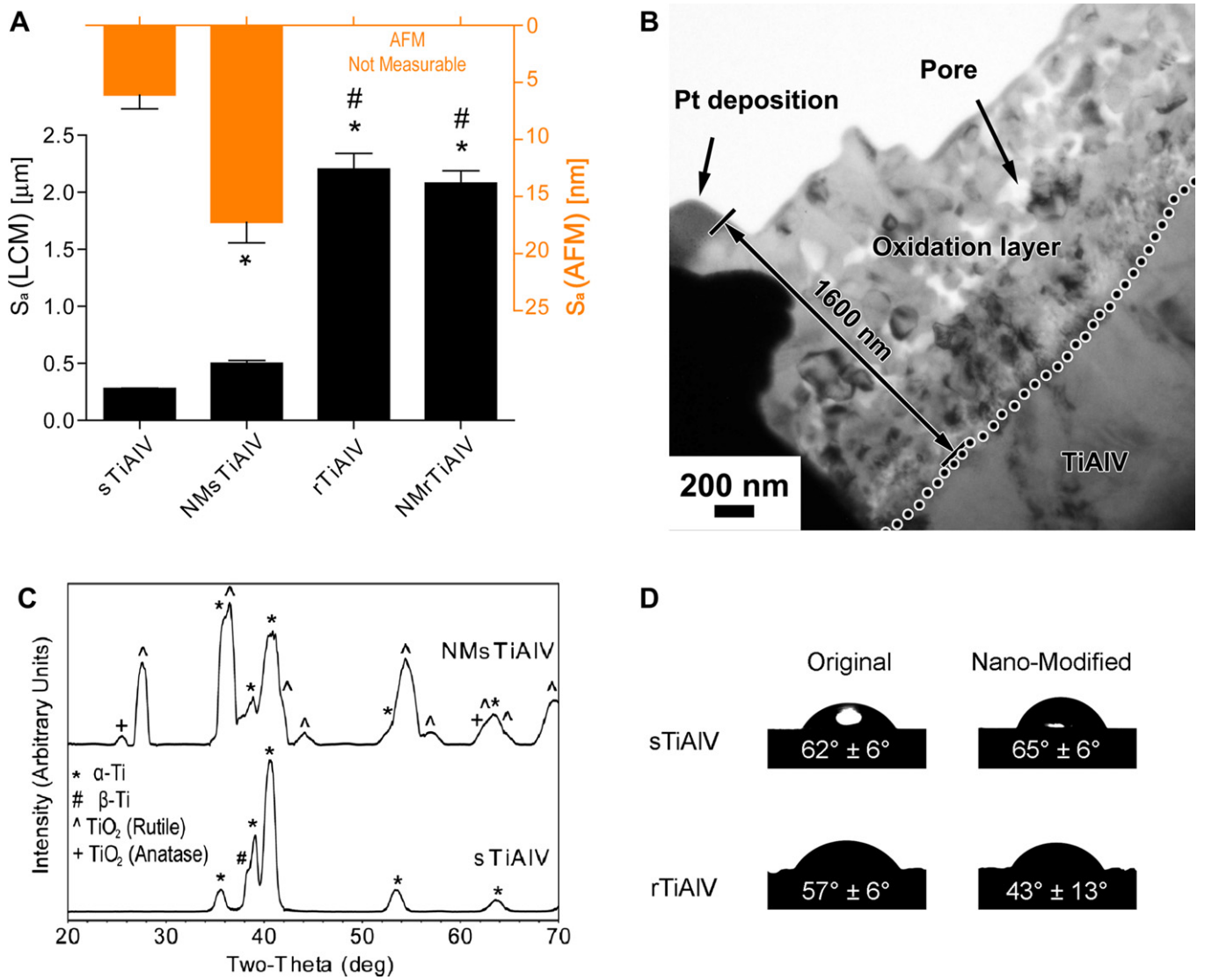

Fig. 3. (A) Surface roughness average (S_a) of sTiAlV and NMsTiAlV surfaces measured by laser confocal microscopy (LCM, black bars) and atomic force microscopy (AFM, orange bars). AFM scans were not possible on microrough specimens, rTiAlV and NMrTiAlV, due to z-height tool limitations. * refers to a statistically-significant p value below 0.05 vs. sTiAlV; # refers to a statistically-significant p value below 0.05 vs. NMsTiAlV. (B) TEM evaluation of an NMsTiAlV surface cross-section prepared by focused ion beam (FIB) milling. The cross-sectional TEM image of the NMsTiAlV specimen reveals a conformal oxide layer that possesses pores and has a thickness of up to 1600 nm (C) X-ray diffraction (XRD) patterns obtained from sTiAlV and NMsTiAlV specimens. The original sTiAlV specimen only exhibited peaks for α- and β-titanium, while the nanomodified NMsTiAlV specimen exhibited peaks for α-titanium, rutile and anatase TiO_2. (D) Sessile-drop water contact angles on the surfaces of sTiAlV, NMsTiAlV, rTiAlV and NMrTiAlV specimens. (For interpretation of the references to color in this figure legend, the reader is referred to the web version of this article.)

sTiAlV specimens, with no further significant enhancement for the NMrTiAlV surfaces. Osteoprotegerin levels (Fig. 5I) on the microrough rTiAlV specimens were 1.5-fold higher when compared to the rest of the specimens, which all had similar levels (even when comparing the microsmooth specimens to the combined microrough and nanostructured NMrTiAlV specimens). In contrast, VEGF production was sensitive to the nanomodification (Fig. 5J). VEGF levels were 1.2-fold higher on the NMsTiAlV surfaces when compared to sTiAlV surfaces, but the highest levels were found on the microrough specimens, with NMrTiAlV surfaces yielding 1.3-fold higher levels than rTiAlV surfaces.

4. Discussion

Surface nanomodification of dental and orthopaedic implants is becoming a common approach to enhance osseointegration [5]. Although several scientific reasons have been postulated for beneficial effects of nanostructures on the surfaces of osseous implants [7], fundamental questions remain to be answered regarding the initial cellular responses to these nanostructural features *in vitro* and *in vivo*. In addition, variations in various parameters of published *in vitro* reports (*e.g.*, the size and nature of the nanostructures evaluated, as well as the phenotype, differentiation stage, and exogenous factors used to culture the cells) provide motivation for direct comparisons of some of these variables [31–33].

In this study, the cellular responses of progenitor and differentiated human osteoblast-lineage cells on the nanomodified surfaces of microsmooth and microrough Ti alloy specimens have been compared to evaluate the cells' abilities to respond to such nanostructures as revealed by the production of osteoblast differentiation markers and release of proteins associated with osteogenesis and vasculogenesis. Our results show that nanostructures can be superimposed on TiAlV surfaces using a simple and effective

Please cite this article in press as: Gittens RA, et al., Differential responses of osteoblast lineage cells to nanotopographically-modified, microroughened titanium–aluminum–vanadium alloy surfaces, Biomaterials (2012), http://dx.doi.org/10.1016/j.biomaterials.2012.08.059

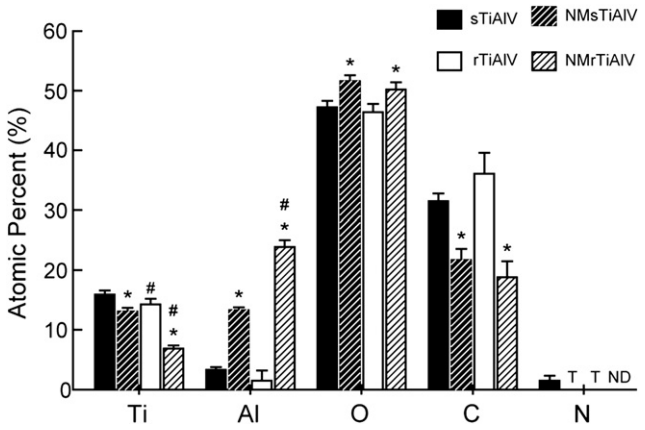

Fig. 4. Elemental compositions of the sTiAlV, NMsTiAlV, rTiAlV and NMrTiAlV specimens measured by XPS. All samples were mainly composed of Ti, Al, and O, with C also highly present on the surface. N was also present at low levels on the sTiAlV surfaces, while NMsTiAlV and rTiAlV surfaces only had traces (T) and on the NMrTiAlV surfaces it was not detectable (ND). * refers to a statistically-significant p value below 0.05 vs. unmodified control; # refers to a statistically-significant p value below 0.05 vs. microsmooth control.

oxidation-based treatment, which had been previously applied to commercially-pure (cp) Ti substrates [11]. However, unlike the TiO_2 surface chemistry generated on the cpTi surface, the nanostructured surface on the alloy had a higher Al content than was present on the unmodified surfaces. As reported previously using the immature MG63 osteoblastic cell line on nanomodified cpTi, HOB cells exhibited a synergistic enhancement in maturation on the nanomodified microrough surfaces, suggesting a greater role for nanotopography over surface chemistry for the maturation of differentiated osteoblast-lineage cells. MSCs on the alloy surfaces responded to microstructure with a less robust osteoblastic response than seen for HOBs on TiAlV and MG63s on the cpTi substrates, and they did not show evidence of further osteoblastic differentiation on the micro/nanostructured alloy surfaces. Instead, the MSCs generated increased VEGF production, indicating sensitivity to the micro/nanostructured surfaces, and suggesting that the surface chemistry could also play a role in determining cell response. These observations are discussed in detail below.

High temperature oxidation in an air atmosphere was used successfully to generate well-defined nanostructures with an average diameter (when viewed from above by SEM analyses) of 60–75 nm, as noted previously for cpTi [11], supporting the general utility of this method for a variety of metal materials. Relatively high and uniform concentrations of such oxidation-induced nanostructures covered the internal and external surfaces of implants with complex shapes (as well as the surfaces of microsmooth and microrough disk-shaped specimens used for *in vitro* studies), proving the clinical and industrial applicability of this treatment. The oxidation-induced nanostructuring of TiAlV alloy surfaces yielded a relatively high density of fine nanostructural features even after just 45 min, and the features remained on the surfaces with low nanostructure coalescence or spallation after longer modification times of 90 and 180 min. This differed from our prior experience with cpTi, which required the longer treatment times to produce a nanostructured surface with comparable morphology [11].

A surface modification process that alters the nanoscale surface roughness while retaining other surface characteristics, allows for reduced ambiguity in assessing the role(s) of such nanoroughness on cell response. With the present oxidation-based process, the surface nanoroughness of Ti alloy specimens was significantly increased, as revealed by AFM and SEM analyses, without significantly degrading the surface microroughness, as measured by LCM analyses. Cross-sectional evaluation of the oxidized alloy surface by TEM analysis revealed that, although the oxide layer was up to 1.6 μm in thickness, the oxide layer conformed with, and remained attached to, the metal surface. The water contact angles of the starting and nanomodified surfaces were also similar, indicating that the surface wettability of the specimens was not greatly affected by the oxidation treatment.

The oxidation-based treatment did result in a chemical alteration of the specimen surfaces, as revealed by XPS analyses. The Al concentration increased, while Ti and C concentrations decreased after the oxidation treatment. The small change in oxygen content detected after oxidation indicated that a thin, native Ti-O-rich scale was present on the starting alloy surfaces, which apparently allowed for similar wetting by water as for the oxidized specimens. No peaks for V were detected in the XPS spectra of the oxidized specimens, as was the case for a previous study evaluating the oxidation of TiAlV samples at lower temperatures and for longer durations [34]. Naturally-passivated Ti–Al alloy specimens tend to form an oxide layer composed almost exclusively of titania [35], whereas high temperature oxidation promotes the formation of an oxide scale with a higher alumina content [36]. Our results were in agreement with the aforementioned studies [35,36]. Furthermore, the temperature of 740 °C used during our heat treatment promoted the formation of an oxide layer containing anatase and rutile titania, as well as an enrichment of aluminum as confirmed by XPS. However, distinct diffraction peaks for crystalline alumina were not detected.

Osteoblast maturation and local factor production were synergistically sensitive to the combined micro/nanostructured TiAlV surfaces, in agreement with our previous study evaluating osteoblast-like MG63 cell response to oxidation-modified, nanostructured Ti grade 2 specimens [11]. Lower osteoblast cell numbers were found on the microrough surfaces, with the lowest levels found on the combined microrough and nanostructured surfaces. Low cell number *in vitro* has commonly been perceived as a negative result with regards to osseointegration [37,38] and has become the problem to be solved in some studies [39,40]. However, the clinical successes of microrough surfaces relative to smoother surfaces that tend to promote proliferation *in vitro* [41], together with reports that have found a transcriptionally-restricted transition between proliferation and differentiation that forces osteoblasts to stop dividing once they start maturing [42], suggest otherwise. Our cell number results, coupled with a synergistically higher production of differentiation markers (especially of the late marker osteocalcin) on the micro- and nanostructured specimens, confirmed that the osteoblasts were maturing and producing the proteins necessary for bone formation. In addition, roughness at the microscale appeared to be more important than nanoscale roughness with regards to controlling the production of the local factor osteoprotegerin, which serves as a decoy receptor for RANKL to inhibit osteoclastogenesis and favor net bone formation. Furthermore, the potent angiogenic factor VEGF, important for neovascularization of the implantation site [43], was strongly influenced by the hierarchically (micro/nano) structured surfaces. These results are also supported by the findings that oxidized TiAlV specimens can increase surface adsorption of key extracellular matrix components such as fibronectin, which could enhance cell response on these combined micro- and nano-modified surfaces [34]. Comparable synergistic maturation responses to nano/microstructured surfaces from HOBs on TiAlV substrates and from immature osteoblast-like MG63 cells on cpTi in our previous study [11], suggests that addition of nanostructures to the underlying microroughness of a substrate plays a more relevant role in the process of osteogenic maturation of differentiated osteoblast-lineage cells than surface chemistry.

Please cite this article in press as: Gittens RA, et al., Differential responses of osteoblast lineage cells to nanotopographically-modified, microroughened titanium–aluminum–vanadium alloy surfaces, Biomaterials (2012), http://dx.doi.org/10.1016/j.biomaterials.2012.08.059

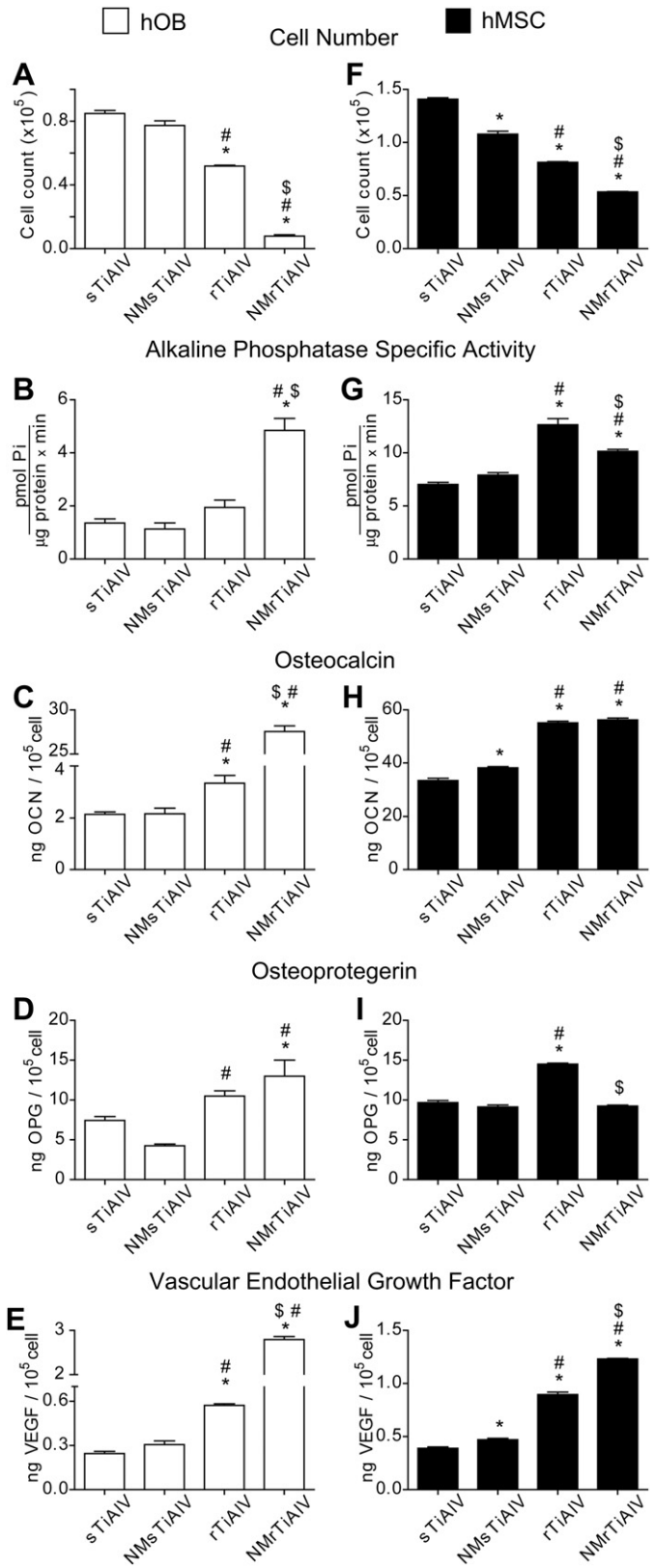

Fig. 5. Effects of micro- and nanoscale surface modifications on human primary osteoblasts (A–E) and human MSCs (F–J). Osteoblasts and MSCs were plated on sTiAlV, NMsTiAlV, rTiAlV and NMrTiAlV surfaces and grown to confluence. The nano-modification involves surface oxidation in flowing synthetic air for 45 min at 740 °C. At confluence, (A, F) cell number, (B, G) alkaline phosphatase specific activity, (C, H) OCN, (D, I) OPG, and (E, J) VEGF levels were measured. Data represented are the mean ± SE of six independent samples. * refers to a statistically-significant p value below 0.05 vs. sTiAlV; # refers to a statistically-significant p value below 0.05 vs. NMsTiAlV; $ refers to a statistically-significant p value below 0.05 vs. rTiAlV.

MSC osteoblastic differentiation was sensitive to microroughness, as seen previously [27], but not sensitive to the nanostructures generated on our Ti alloys. Cell number was lower on the microrough surfaces than on the microsmooth surfaces, as was the case for the osteoblasts. Moreover, the production of differentiation markers was also enhanced on the microrough Ti alloy surfaces relative to microsmooth surfaces, which confirmed the influence of microroughness on the enhanced differentiation of MSCs [27,44]. The lowest MSC numbers were found on the micro/nanostructured surfaces, which suggested that osteogenic differentiation was induced. However, MSCs growing on the combined microrough and nanostructured surfaces had lower alkaline phosphatase specific activity and produced similar osteocalcin levels than those growing on only microrough surfaces. The lower levels in alkaline phosphatase specific activity and equal levels of osteocalcin on the combined micro/nanostructured surfaces compared to the microrough-only surfaces suggest that these cells were not responding to the nanostructures via osteoblastic differentiation. An alternative explanation is that MSC differentiation was accelerated and the peak in osteocalcin production had been reached on both the microrough and combined micro/nanorough surfaces. However, contrary to the latter conclusion is the fact that most of the studies evaluating micro/nanostructured surfaces have used osteogenic media with soluble factors, such as dexamethasone and β-glycerophosphate, to force the osteogenic differentiation of the stem cells, and these studies still found a higher expression of differentiation markers compared to microrough control surfaces [5,32,45]. In such cases, the exogenous factors used can effectively turn the MSCs into osteoblasts, which we have shown here do respond synergistically to the nanostructures on the Ti alloy. It is clear that MSCs and HOBs were differentially regulated by the surface, not only with respect to robustness of the response but also with respect to osteoprotegerin production. One other study compared human MSC and HOB response to nanostructured TiAlV substrates, without adding osteogenic media, using grooved, relatively microsmooth surfaces [46]. The authors found that MSCs were more sensitive to the nanogrooves than HOBs in terms of cell proliferation and cell viability, in agreement with the results reported in the present study. No other study, to our knowledge, has evaluated the response of MSCs to physiologically- and clinically-relevant, micro/nanostructured TiAlV surfaces without the addition of osteogenic soluble factors, which could explain the lack of understanding of the genuine *in vitro* response of these cells.

A comparison of the results obtained in this study between osteoblast-lineage cells at distinct differentiation stages revealed that primary osteoblasts were able to recognize the surface nanostructures and respond to them with a synergistic production of factors related to osteogenic maturation. Conversely, MSC osteoblastic differentiation was not as sensitive to the nanostructures, as evidenced by the lower-to-similar production of osteogenic markers on the combined micro/nanostructured surfaces compared to the micro-rough surfaces. Our results show that MSCs were indeed responsive to the nanostructures formed on the Ti alloy or to the surface chemistry, as seen in cell number and VEGF production assays. The relatively low sensitivity of MSC osteoblastic differentiation towards these oxidation-induced nanostructures, coupled with reports showing the beneficial role of nanomodified implants *in vivo* [12,47,48], may indirectly suggest that, even if these stem cells were the first to approach the implant *in vivo*, they might already be committed to a specific lineage by the time they reach the surface.

Please cite this article in press as: Gittens RA, et al., Differential responses of osteoblast lineage cells to nanotopographically-modified, microroughened titanium–aluminum–vanadium alloy surfaces, Biomaterials (2012), http://dx.doi.org/10.1016/j.biomaterials.2012.08.059

5. Conclusions

The present paper demonstrates that the differentiation state of osteoblast-lineage cells can determine their response to oxidation-induced surface nanostructures on a titanium alloy in terms of the production of osteoblast differentiation markers, which has implications for clinical evaluation of new implant surface nano-modifications. The osteoblastic differentiation of primary human osteoblasts but not osteoblastic differentiation of MSCs was highly sensitive to nanostructures superimposed by oxidation onto microrough Ti alloy surfaces in the absence of any exogenous soluble factors. In contrast, MSCs responded to the nanostructured microrough surfaces with increased production of angiogenic factors. These findings support the conclusion that the successful osseointegration of an implant depends on contributions from osteoblast lineage cells at different stages of osteoblast commitment and indicates the importance of examining cell response in multiple *in vitro* models.

Acknowledgments

This research was supported by USPHS AR052102 and the ITI Foundation. RAG is partially supported by a fellowship from the Government of Panama (IFARHU-SENACYT). Support for the work of TM and YC was provided by the U.S. Air Force Office of Scientific Research (Award No. FA9550-09-1-0162). Support for the work of KHS was provided by the U.S. Department of Energy, Office of Basic Energy Sciences (Award No. DE-SC0002245). The sTiAlV and rTiAlV specimens as well as the Endoskeleton® TT implants were provided by Titan Spine LLC. The authors thank Prof. Rina Tannenbaum for her advice and support.

Appendix A. Supplementary data

Supplementary data related to this article can be found at http://dx.doi.org/10.1016/j.biomaterials.2012.08.059.

References

[1] Jacobs JJ, Andersson GBJ, Bell JE, Weinstein SL, Dormans JP, Gnatz SM, et al. United States bone and joint decade: the burden of musculoskeletal diseases in the United States. 1st ed. Rosemont: AAOS; 2008.
[2] Fransson C, Wennstrom J, Berglundh T. Clinical characteristics at implants with a history of progressive bone loss. Clin Oral Implants Res 2008;19(2):142–7.
[3] Granstrom G. Osseointegration in irradiated cancer patients: an analysis with respect to implant failures. J Oral Maxillofac Surg 2005;63(5):579–85.
[4] Rho JY, Kuhn-Spearing L, Zioupos P. Mechanical properties and the hierarchical structure of bone. Med Eng Phys 1998;20(2):92–102.
[5] Kubo K, Tsukimura N, Iwasa F, Ueno T, Saruwatari L, Aita H, et al. Cellular behavior on TiO_2 nanonodular structures in a micro-to-nanoscale hierarchy model. Biomaterials 2009;30(29):5319–29.
[6] Geblinger D, Addadi L, Geiger B. Nano-topography sensing by osteoclasts. J Cell Sci 2010;123(9):1503–10.
[7] Mulari MTK, Qu Q, Harkonen PL, Vaananen HK. Osteoblast-like cells complete osteoclastic bone resorption and form new mineralized bone matrix in vitro. Calcif Tissue Int 2004;75(3):253–61.
[8] Boyan BD, Schwartz Z, Lohmann CH, Sylvia VL, Cochran DL, Dean DD, et al. Pretreatment of bone with osteoclasts affects phenotypic expression of osteoblast-like cells. J Orthop Res 2003;21(4):638–47.
[9] Parfitt AM. The vascular contribution to bone remodeling. J Bone Miner Res 2000;15(4):823.
[10] Wennerberg A, Albrektsson T. Effects of titanium surface topography on bone integration: a systematic review. Clin Oral Implants Res 2009;20:172–84.
[11] Gittens RA, McLachlan T, Olivares-Navarrete R, Cai Y, Berner S, Tannenbaum R, et al. The effects of combined micron-/submicron-scale surface roughness and nanoscale features on cell proliferation and differentiation. Biomaterials 2011;32(13):3395–403.
[12] Tsukimura N, Ueno T, Iwasa F, Minamikawa H, Sugita Y, Ishizaki K, et al. Bone integration capability of alkali- and heat-treated nanobimorphic Ti-15Mo-5Zr-3Al. Acta Biomater 2011;7(12):4267–77.
[13] Orsini G, Piattelli M, Scarano A, Petrone G, Kenealy J, Piattelli A, et al. Randomized, controlled histologic and histomorphometric evaluation of implants with nanometer-scale calcium phosphate added to the dual acid-etched surface in the human posterior maxilla. J Periodontol 2007;78(2):209–18.
[14] Collaert B, Wijnen L, De Bruyn H. A 2-year prospective study on immediate loading with fluoride-modified implants in the edentulous mandible. Clin Oral Implants Res 2011;22(10):1111–6.
[15] Isa ZM, Schneider GB, Zaharias R, Seabold D, Stanford CM. Effects of fluoride-modified titanium surfaces on osteoblast proliferation and gene expression. Int J Oral Maxillofac Implants 2006;21(2):203–11.
[16] Giavaresi G, Fini M, Chiesa R, Giordano C, Sandrini E, Bianchi AE, et al. A novel multiphase anodic spark deposition coating for the improvement of orthopedic implant osseointegration: an experimental study in cortical bone of sheep. J Biomed Mater Res A 2008;85(4):1022–31.
[17] Jimbo R, Xue Y, Hayashi M, Schwartz HO, Andersson M, Mustafa K, et al. Genetic responses to nanostructured calcium-phosphate-coated implants. J Dent Res 2011;90(12):1422–7.
[18] Kokubo T, Kim HM, Kawashita M, Nakamura T. Bioactive metals: preparation and properties. J Mater Sci Mater Med 2004;15(2):99–107.
[19] Crawford GA, Chawla N, Das K, Bose S, Bandyopadhyay A. Microstructure and deformation behavior of biocompatible TiO_2 nanotubes on titanium substrate. Acta Biomater 2007;3(3):359–67.
[20] MacDonald DE, Rapuano BE, Schniepp HC. Surface oxide net charge of a titanium alloy: comparison between effects of treatment with heat or radio-frequency plasma glow discharge. Colloids Surf B Biointerfaces 2011;82(1):173–81.
[21] Richert L, Variola F, Rosei F, Wuest JD, Nanci A. Adsorption of proteins on nanoporous Ti surfaces. Surf Sci 2010;604(17–18):1445–51.
[22] Davies JE. In vitro modeling of the bone/implant interface. Anat Rec 1996;245(2):426–45.
[23] Dalby MJ, Gadegaard N, Tare R, Andar A, Riehle MO, Herzyk P, et al. The control of human mesenchymal cell differentiation using nanoscale symmetry and disorder. Nat Mater 2007;6(12):997–1003.
[24] Mendonca DBS, Miguez PA, Mendonca G, Yamauchi M, Aragao FJL, Cooper LF. Titanium surface topography affects collagen biosynthesis of adherent cells. Bone 2011;49(3):463–72.
[25] You MH, Kwak MK, Kim DH, Kim K, Levchenko A, Kim DY, et al. Synergistically enhanced osteogenic differentiation of human mesenchymal stem cells by culture on nanostructured surfaces with induction media. Biomacromolecules 2010;11(7):1856–62.
[26] Boyan BD, Bonewald LF, Paschalis EP, Lohmann CH, Rosser J, Cochran DL, et al. Osteoblast-mediated mineral deposition in culture is dependent on surface microtopography. Calcif Tissue Int 2002;71(6):519–29.
[27] Olivares-Navarrete R, Hyzy SL, Hutton DL, Erdman CP, Wieland M, Boyan BD, et al. Direct and indirect effects of microstructured titanium substrates on the induction of mesenchymal stem cell differentiation towards the osteoblast lineage. Biomaterials 2010;31(10):2728–35.
[28] Olivares-Navarrete R, Hyzy SL, Chaudhri RA, Zhao G, Boyan BD, Schwartz Z. Sex dependent regulation of osteoblast response to implant surface properties by systemic hormones. Biol Sex Differ 2010;1(1):4.
[29] Bretaudiere JP, Spillman T. Alkaline phosphatases. Weinheim, Germany: Verlag Chemica; 1984.
[30] Boyan BD, Batzer R, Kieswetter K, Liu Y, Cochran DL, Szmuckler-Moncler S, et al. Titanium surface roughness alters responsiveness of MG63 osteoblast-like cells to 1 alpha,25-(OH)(2)D-3. J Biomed Mater Res 1998;39(1):77–85.
[31] Zhao L, Mei S, Chu PK, Zhang Y, Wu Z. The influence of hierarchical hybrid micro/nano-textured titanium surface with titania nanotubes on osteoblast functions. Biomaterials 2010;31(19):5072–82.
[32] Mendonca G, Mendonca DBS, Aragao FJL, Cooper LF. The combination of micron and nanotopography by H_2SO_4/H_2O_2 treatment and its effects on osteoblast-specific gene expression of hMSCs. J Biomed Mater Res A 2010;94A(1):169–79.
[33] Wilkinson A, Hewitt RN, McNamara LE, McCloy D, Dominic Meek RM, Dalby MJ. Biomimetic microtopography to enhance osteogenesis in vitro. Acta Biomater 2011;7(7):2919–25.
[34] MacDonald DE, Rapuano BE, Deo N, Stranick M, Somasundaran P, Boskey AL. Thermal and chemical modification of titanium-aluminum-vanadium implant materials: effects on surface properties, glycoprotein adsorption, and MG63 cell attachment. Biomaterials 2004;25(16):3135–46.
[35] Luthra KL. Stability of protective oxide-films on ti-base alloys. Oxid Met 1991;36(5–6):475–90.
[36] Du HL, Datta PK, Lewis DB, Burnellgray JS. Air oxidation behavior of Ti-6Al-4V alloy between 650-degrees-C and 850-degrees-C. Corros Sci 1994;36(4):631–42.
[37] Aita H, Hori N, Takeuchi M, Suzuki T, Yamada M, Anpo M, et al. The effect of ultraviolet functionalization of titanium on integration with bone. Biomaterials 2009;30(6):1015–25.
[38] Saito T, Hayashi H, Kameyama T, Hishida M, Nagai K, Teraoka K, et al. Suppressed proliferation of mouse osteoblast-like cells by a rough-surfaced substrate leads to low differentiation and mineralization. Mater Sci Eng C Mater Biol Appl 2010;30(1):1–7.
[39] Pittrof A, Park J, Bauer S, Schmuki P. ECM spreading behaviour on micro-patterned TiO(2) nanotube surfaces. Acta Biomater 2012;8(7):2639–47.
[40] Webster TJ, Ejiofor JU. Increased osteoblast adhesion on nanophase metals: Ti, Ti6Al4V, and CoCrMo. Biomaterials 2004;25(19):4731–9.
[41] Cochran DL. A comparison of endosseous dental implant surfaces. J Periodontol 1999;70(12):1523–39.

[42] Stein GS, Lian JB, Stein JL, VanWijnen AJ, Montecino M. Transcriptional control of osteoblast growth and differentiation. Physiol Rev 1996;76(2):593–629.
[43] Raines AL, Olivares-Navarrete R, Wieland M, Cochran DL, Schwartz Z, Boyan BD. Regulation of angiogenesis during osseointegration by titanium surface microstructure and energy. Biomaterials 2010;31(18):4909–17.
[44] Wall I, Donos N, Carlqvist K, Jones F, Brett P. Modified titanium surfaces promote accelerated osteogenic differentiation of mesenchymal stromal cells in vitro. Bone 2009;45(1):17–26.
[45] Khang D, Choi J, Im YM, Kim YJ, Jang JH, Kang SS, et al. Role of subnano-, nano- and submicron-surface features on osteoblast differentiation of bone marrow mesenchymal stem cells. Biomaterials 2012;33(26):5997–6007.
[46] Calzado-Martin A, Mendez-Vilas A, Multigner M, Saldana L, Gonzalez-Carrasco JL, Gonzalez-Martin ML, et al. On the role of RhoA/ROCK signaling in contact guidance of bone-forming cells on anisotropic Ti6Al4V surfaces. Acta Biomater 2011;7(4):1890–901.
[47] Bjursten LM, Rasmusson L, Oh S, Smith GC, Brammer KS, Jin S. Titanium dioxide nanotubes enhance bone bonding in vivo. J Biomed Mater Res A 2010; 92(3):1218–24.
[48] Mendonca G, Mendonca DBS, Simoes LGP, Araujo AL, Leite ER, Golin AL, et al. Nanostructured implant surface effect on osteoblast gene expression and bone-to-implant contact in vivo. Mater Sci Eng C Mater Biol Appl 2011;31(8): 1809–18.

Please cite this article in press as: Gittens RA, et al., Differential responses of osteoblast lineage cells to nanotopographically-modified, microroughened titanium–aluminum–vanadium alloy surfaces, Biomaterials (2012), http://dx.doi.org/10.1016/j.biomaterials.2012.08.059